12th International Conference on Advances in Steel-Concrete Composite Structures (ASCCS 2018)
Universitat Politècnica de València, València, Spain, June 27-29, 2018
Doi: http://dx.doi.org/10.4995/ASCCS2018.2018.7287

Hysteretic performance research on high strength circular concrete-filled thin-walled steel tubular columns

Jiantao Wang[a], Qing Sun[a]*

[a]Department of Civil Engineering, Xi'an Jiaotong University, China
*corresponding author, e-mail address: sunq@mail.xjtu.edu.cn

Abstract

Under violent earthquake motions, the severe damage in critical regions of structures could be ascribed to cumulative damage caused by cyclic loading. Using the high strength (HS) materials in concrete-filled steel tubular (CFST) columns is the effective way and popular tendency to promote the seismic behavior in anti-seismic design. In this paper, an experimental study on the hysteretic performance of high strength circular concrete-filled thin-walled steel tubular columns (HCFTST) columns was carried out. A total of six specimens were tested under constant axial compression combining cyclic lateral loading. The tested parameters were the different combinations of diameter-to-thickness (D/t) ratio, axial compression ratio (n) and concrete cylinder compressive strength (f_c).The failure modes, load-displacement hysteretic curves, skeleton curves, dissipated energy and stiffness degradation were examined in detail. Through the experiment analysis result, it indicates that the ultimate limit state is reached as the severe local buckling and rupture of the steel tubes accompanying the core concrete crushing occur. Using high strength materials could have a larger elastic deformation capacity and the higher axial compression ratio within test scopes could motivate the potential of HS materials. In brief, the HCFTST columns with ultra-large D/t ratios under reasonable design could perform excellent hysteretic performance, which can be applied in earthquake-prone regions widely.

Keywords: *High strength circular concrete-filled thin-walled steel tubular (HCFTST) columns; hysteretic performance; failure modes;experiment analysis.*

1. Introduction

Concrete-filled steel tubular (CFST) columns as a relatively new type of structural member, have been widely applied in engineering construction, not only due to their remarkable mechanical properties for seismic resistance, namely the high strength, large lateral stiffness, high ductility and greater energy dissipation capacity, but also due to its outstanding construction efficiency and economic benefits [1-3]. Earlier significant experimental researches conducted by many scholars [4-14] do have great importance on the understanding of hysteretic performance of CFST columns. Recently, using the high strength (HS) materials in concrete-filled steel tubular (CFST) columns is the effective way and popular tendency to promote the seismic behavior in anti-seismic design [15-18].

Elremaily and Azizinamini [15] carried out experimental study on cyclic behavior of circular CFST columns with concrete cylinder compressive strength (f_c) varying from 40 to 104 MPa. Varma et al. [16, 17] examined the seismic behavior of HS square CFST columns filled with HS concrete (f_c =110 MPa) and steel yield strength (f_y) ranging from 269 to 660 MPa. Skalomenos et al. [18] investigated the hysteretic behavior of circular and square CFST columns with f_c varying from 42.4 to 82.3 MPa and f_y varying from 387 to 788 MPa. For the CFST columns, the HS steel tube can provide a larger elastic deformation capacity and better confined effect, while the application of HS core concrete can delay local buckling of steel tube. Moreover, using HS concrete and common strength (CS) steel, using HS steel and CS concrete or both materials are HS, can reduce the section size to obtain favorable architecture aesthetics effect

and gain further economic benefits under the premise of ensuring the mechanical performance [19].

High strength circular concrete-filled thin-walled steel tubular (HCFTST) columns get rapid development due to the widespread application of HS materials. As for the concrete-filled thin-walled steel tubular (CFTST) columns, Zhang et al. [20], Goto et al. [21] and Gajalakshmi [22] investigated the hysteretic behavior of that through quasi-static cyclic loading tests. However, it is noteworthy that no HS materials were adopted in their tests [20-22]. On the other hand, the aforementioned researches [15-18] mainly aim at hysteretic behavior of the traditional concrete-filled thick-walled steel tubular columns using HS materials. Therefore, more experimental studies are needed to examine the hysteretic performance of CFTST columns using HS materials, namely the HCFTST columns.

In this paper, an experimental study on the hysteretic performance of HCFTST columns, including six specimens, was carried out under constant axial compression combining cyclic lateral loading. The tested parameters were the different combinations of diameter-to-thickness (D/t) ratio, axial compression ratio (n) and concrete cylinder compressive strength (f_c). The failure modes, load-displacement hysteretic curves, skeleton curves, dissipated energy and stiffness degradation were examined in detail. Overall, the HCFTST columns with reasonable design could display favorable hysteretic performance.

2. Experimental program

2.1. Material properties

The reserved concrete blocks for compressive strength test were curing under the same condition with test columns. The actual cylinder strengths (f_c) are listed in Table 1. The Q690 HS steel was used to make the steel tubes. Tensile coupon test shown in Fig. 1, according to "Metallic materials tensile testing at ambient temperature" (GB/T 228-2002), was carried out to determine the material properties. The test result shows that the yield strength f_y is 722.64 MPa and ultimate strength f_u is 765.37 MPa. The elastic modulus E_s is 222010 Mpa and the Poisson's ratio v_s is 0.281.

Table 1. Actual strength of concrete

Grade	f_c (Mpa)
CS-1	43.5
CS-2	49.1
HS-1	78.6
HS-2	97.6

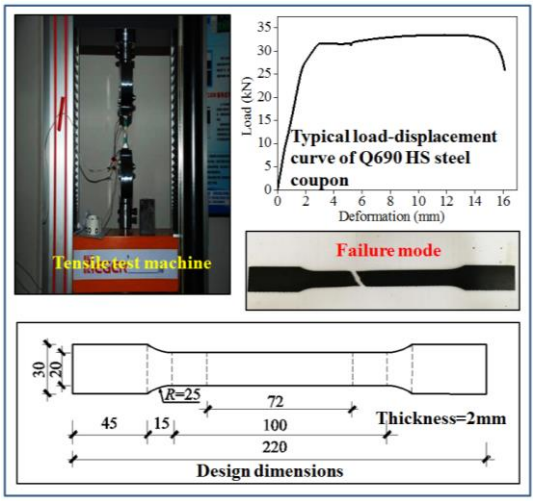

Fig. 1. Coupon tensile test

2.2. Specimen design

A summary of specimens is presented in Table 2, in which the D/t ratios adopted exceeds the current limitations specified by various codes [22] to examine the effect of it. The axial compression ratio (n) in this paper is defined as follows:

$$n = P / P_0 \tag{1}$$

where P is the axial load applied on the HCFTST columns and P_0 is the nominal squash load calculated by the equation as follows:

$$P_0 = A_s f_y + 0.85 A_c f_c \tag{2}$$

where A_s and A_c are the cross-sectional areas of the steel tube and concrete core respectively.

The designed details of all aforementioned test specimens are shown in Fig. 2. The height of the HCFTST columns is 525 mm and a reinforced concrete (RC) foundation was built for the convenience of applying cyclic loads. The thickness of all end plates is 20 mm, especially for end plates II with bolt holes welded at the top of specimen for loading. The cross section sizes of the RC foundation are $1200(\text{length}) \times 450(\text{width}) \times 420(\text{height})$ mm and $1200 \times 500 \times 420$ mm, where the former was adopt by the HCFTST columns with diameters 140 mm and 180mm, and the later was

applied to the other specimens. HS steel bars (f_y=1000MPa) were used to prevent the RC foundations out of failure during test. Furthermore, stiffening ribs with a thickness of 10 mm were also applied by welding to strengthen the foundations.

Table 2. Summary of specimens

No.	*D/t*	f_c (mm)	*n*
CFST-1-1	140/2	78.6	0.27
CFST-1-2	140/2	97.6	0.36
CFST-2-1	180/2	43.5	0.18
CFST-2-2	180/2	97.6	0.27
CFST-3-1	220/2	49.1	0.36
CFST-3-2	220/2	97.6	0.18

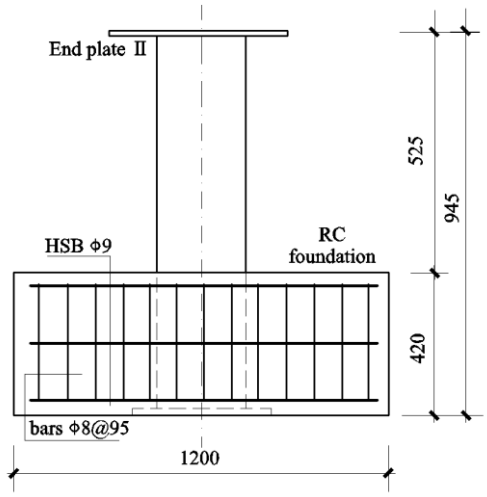

Fig. 2. Specimens details

2.3. Test setup and procedures

The loading apparatus adopted for the test shown in Fig. 3 enables the application of the constant axial compressive load combining cyclic lateral load. The axial compression was imposed on the column attached with the triangular box connector through a hydraulic jack of 2000 kN capacity and the 1000 kN loading capacity MTS 244.51 actuator was used to apply cyclic lateral load. In addition, the connector, test columns and actuator were fixed together by HS bolts Grade 12.9 M28. Furthermore, to ensure the stability of test specimen, the RC foundation was attached to the ground tightly with pressure beams and anchor stocks while two adjustable seats were installed to prevent the lateral sliding of the specimen. The horizontal load and displacement were automatically recorded by the MTS actuator acting on the test columns. The axial force was monitored by the pressure transducers fixed on the jack.

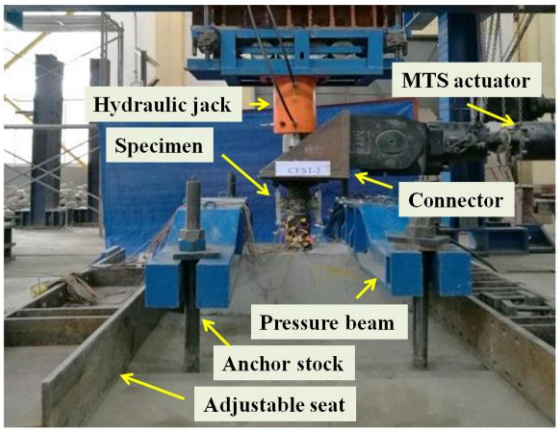

Fig. 3. Test setup

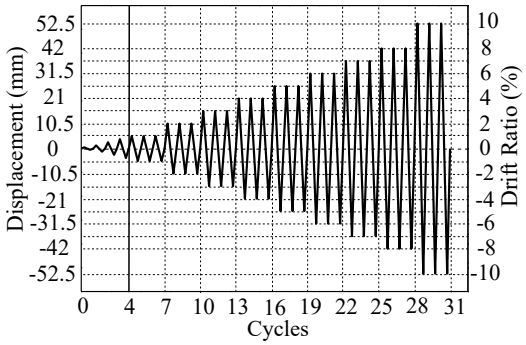

Fig. 4. Cyclic loading protocol

During the test, preloading procedure was conducted to ensure the equipment ran normally. If all was in order, the axial load was applied firstly to the targeted value and then kept constant during testing. Afterwards the lateral force was cycled under the displacement control mode as shown in Fig. 4. Four single cycles with peak drift ratios of $\Delta / L = 0.10\%$, 0.25%, 0.50% and 0.75% were initially applied, where 'Δ' indicates the lateral displacement and 'L' stands for the column length. Then three cycles were employed to the specimen at each drift ratio level from 1% to 8%. What's more, if there was no evident failure occurring after applying drift ratio 8%, the test would continue by applying drift ratio 10% until the specimen failed. The test ended when the specimen was unable to sustain the targeted axial force due to the severe fracture and crushing of the steel tube and core concrete or the lateral load degraded over than 35% of the maximum experienced load.

3. Failure modes

The typical events including slight local buckling, severe buckling before fracture, crack appearing without penetrating tube and serious accompanied with rupture almost penetrating cross section occurred during the test. A summary of failure modes for HCFTST columns is shown in Fig. 5. As is shown, the severe fracture and local buckling of thin-walled steel tubes could be observed apparently in the end. For all test columns, the cracking height is about 20 mm away from the RC foundation surface. After the test, the specimen CFST-3-2 with the severest cross section failure was cut off to examine the failure mode of core concrete. Apparently, the core concrete experienced serious damage under the cyclic loading. Moreover, the confined effect decreased gradually due to the local buckling occurring, for which the HS core concrete of the test column finally underwent an adverse shear failure mode with a smooth fracture surface.

Fig. 5. Failure modes

4. Experimental analysis

4.1. Load-displacement hysteretic curves

The load-displacement hysteretic curves of all test columns are shown in the plots as follows. It indicates that there is an initial elastic response for all specimens and then the columns enter the elastic-plastic process accompanied by the increasing stiffness degradation and energy dissipation gradually. The initial local buckling points and fracture of steel tube are marked in the curves. Generally the initial local buckling occurred at drift ratio 2%~3% for most specimens and the fracture of steel tube emerged until reaching the 7%~8% drift. A gradual drop in strength can be seen when maximum lateral load is reached. The hysteretic curves are not strictly symmetrical because during the reciprocating loading cumulative damage develops preferentially due to the initial imperfections of the HS material and obvious Bauschinger effect of HS steel. For the other HCFTST columns, with the increasing of drift level, there are obvious softening platforms existing in hysteretic curves when the lateral load turns from unloading to reloading. For HCFTST columns with ultra-large D/t ratio exceeding current codes, increasing axial compression ratio is an efficient way than improving concrete strength to motivate the potential of HS materials for offering an excellent confined action to limit the propagation of the concrete shear cracks in anti-seismic design.

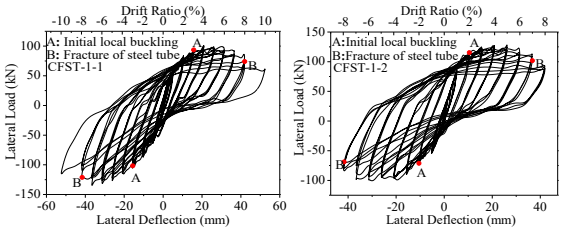

Fig. 6. CFST-1-1 and CFST-1-2

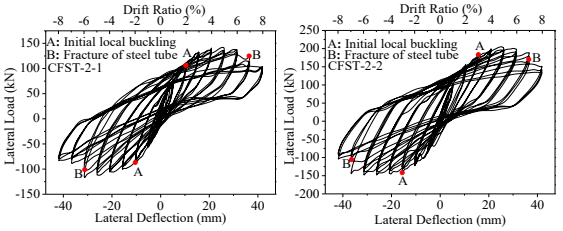

Fig. 7. CFST-2-1 and CFST-2-2

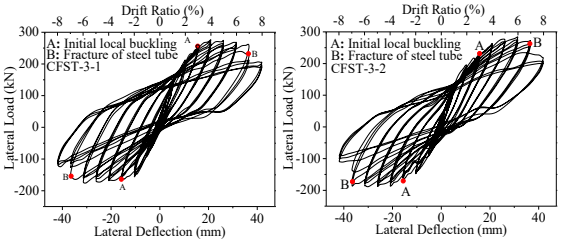

Fig. 8. CFST-3-1 and CFST-3-2

4.2. Energy dissipation capacity

The energy dissipation analysis was conducted by the area integral based on the hysteretic curves, as shown in Fig. 9, from which it indicates that the loop energy of different drift levels amplifies gradually with the

increasing of lateral deflection level while within the same drift deformation the loop energy decreases gradually due to the cumulative damage caused by cyclic loading. when entering the failure stage, the evident descending of loop energy could be observed revealing that the tested specimens would fail soon later. As for the accumulated energy ratio, it can be expressed as follows:

$$R_{Ei} = \sum_{i=1}^{n} E_i / E_T \tag{3}$$

where E_i is the accumulated energy until the cyclic loop n and E_T is the total ultimate energy dissipation. Fig. 10 shows the result of accumulatived energy ratio analysis, which display that the cumulative damage develops in a nonlinear way with starting slowly and then converts to a burgeoning mode after the appearance of initial local buckling.

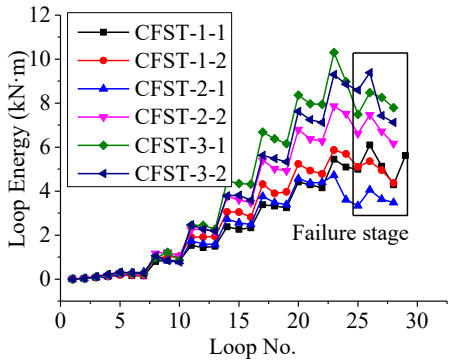

Fig. 9. Energy dissipation analysis

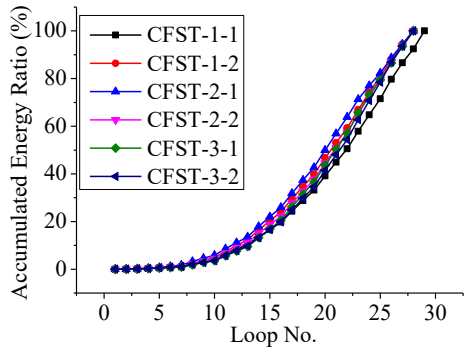

Fig. 10. Accumulated energy ratio analysis

The energy dissipation capacity could also be evaluated by the equivalent viscous damping coefficient shown in Fig. 11, which can be calculated through the equation:

$$h_e = \frac{S_{(ABC+CDA)}}{2\pi S_{(\Delta OBF+\Delta ODE)}} \tag{4}$$

where $S_{(ABC+CDA)}$ is the area of hysteretic loop and $S_{(\Delta OBF+\Delta ODE)}$ is the area of triangles. The analysis of equivalent viscous damping ratio is displayed in Fig. 12. The result reiterates the fact that the energy dissipation capacity of the HCFTST columns decreases obviously in the failure stage due to the rupture of the thin-wallled steel tubes and concrete crushing.

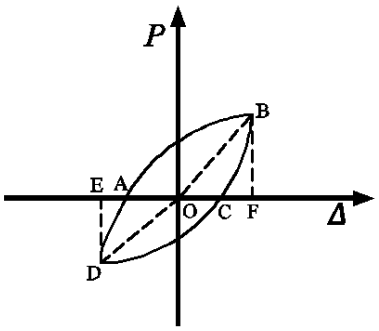

Fig. 11. Equivalent viscous damp ratio

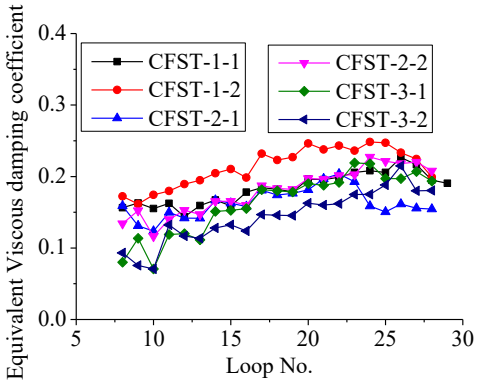

Fig. 12. Equivalent viscous damping ratio

4.3. Skeleton curves

The skeleton curves of tested specimens shown in Fig. 13 were constructed by connecting maximum load point at each displacement level according to the load-displacement hysteretic curves. From the skeleton curves, improving the concrete strength and axial compression ratio within the test scope, can promote the the ultimate bearing capacity of HCFTST columns. For the columns with ultra-large *D*/*t* ratio, improving the axial load level could motivate the potential of the HS materials due to the better workability of confined effect.

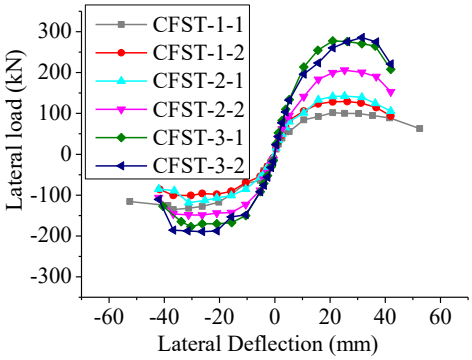

Fig. 13. Skeleton curves

4.4. Stiffness degradation

In this test, linear fit method was employed to calculate the tangent stiffness for all loops at different drift ratios of all tested columns during the unloading. The summary of unified tangent stiffness for all tested specimens is shown in Fig. 14, in which the gradual degradation of stiffness could be observed apparently due to the local buckling and concrete crushing. All that describes the basic propagation of cumulative damage under reciprocating incremental lateral load mode.

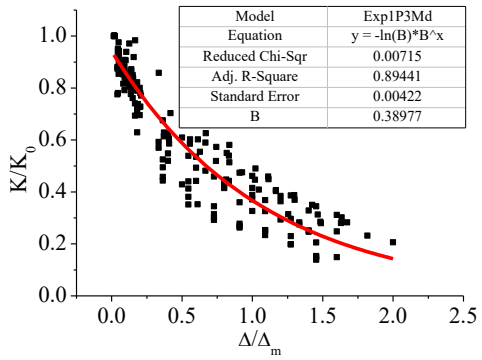

Fig. 14. Stiffness degradation

5. Conclusions

This paper presents the experimental study on hysteretic performance of HCFTST columns. Based on the experimental results, the following conclusions can be drawn within the scope of the current study:

(1) The failure mode of HCFTST columns was reached as the severe local buckling and fracture of steel tube accompanied the core concrete crushing at 7%~8% drift ratio. For HCFTST columns with ultra-large *D*/*t* ratio exceeding current codes, increasing axial compression ratio is an efficient way than improving concrete strength to motivate the potential of HS materials for offering an excellent confined action to limit the propagation of the concrete shear cracks in anti-seismic design.

(2) The evident descending of energy dissipation could be observed in failure stage, indicating forthcoming severe failure phenomenon, namely the complete fracture of steel tube and severe crushing of core concrete.

(3) The HCFTST columns with reasonable design could display favorable hysteretic performance and can be expected to have a widespread application in earthquake-prone regions.

References

[1] Varma A H, Ricles J M, Sause R, et al. Seismic behavior and modeling of high-strength composite concrete-filled steel tube (CFT) beam–columns. Journal of Constructional Steel Research 2002; 58(5): 725-758.

[2] Sakino K, Nakahara H, Morino S, et al. Behavior of centrally loaded concrete-filled steel-tube short columns. Journal of Structural Engineering 2004; 130(2): 180-188.

[3] Liao F Y, Han L H, Tao Z. Behaviour of composite joints with concrete encased CFST columns under cyclic loading: Experiments. Engineering Structures 2014; 59: 745-764.

[4] Sakino K, Tomii M. Hysteretic behavior of concrete filled square steel tubular beam-columns failed in flexure. Transactions of the Japan Concrete Institute 1981; 3(6): 439-446.

[5] Morishita Y, Tomii M. Experimental studies on bond strength between square steel tube and encased concrete core under cyclic shearing force and constant axial force. Transactions of Japan Concrete Institute 1982; 4: 363-370.

[6] Boyd P F, Cofer W F, Mclean D I. Seismic performance of steel-encased concrete columns under flexural loading. ACI Structural Journal 1995; 92(3): 355-364.

[7] Usami T, Ge H. Ductility of concrete-filled steel box columns under cyclic loading. Journal of structural engineering 1994; 120(7): 2021-2040.

[8] Hajjar J F, Gourley B C. A Cyclic Nonlinear Model for Concrete-Filled Tubes. I: Formulation. Journal of Structural Engineering 1997; 123(6):736-744.

[9] Lahlou K, Lachemi M, Aïtcin P C. Confined high-strength concrete under dynamic compressive loading. Journal of Structural Engineering 1999; 125(10): 1100-1108.

[10] Nakanishi K, Kitada T, Nakai H. Experimental study on ultimate strength and ductility of concrete filled steel columns under strong earthquake. Journal of Constructional Steel Research 1999; 51(3): 297-319.

[11] Fam A, Qie F S, Rizkalla S. Concrete-filled steel tubes subjected to axial compression and lateral cyclic loads. Journal of Structural Engineering 2004; 130(4): 631-640.

[12] Marson J, Bruneau M. Cyclic testing of concrete-filled circular steel bridge piers having encased fixed-based detail. Journal of Bridge Engineering 2004; 9(1): 14-23.

[13] Han L H, Huang H, Tao Z, et al. Concrete-filled double skin steel tubular (CFDST) beam–columns subjected to cyclic bending. Engineering Structures 2006; 28(12):1698-1714.

[14] Lehman D E, Kuder K G, Gunnarrson A K, et al. Circular Concrete-Filled Tubes for Improved Sustainability and Seismic Resilience. Journal of Structural Engineering 2015; 141(3):B4014008.

[15] Elremaily A, Azizinamini A. Behavior and strength of circular concrete-filled tube columns. Journal of Constructional Steel Research 2002; 58(12):1567-1591.

[16] Varma A H, Ricles J M, Sause R, et al. Experimental Behavior of High Strength Square Concrete-Filled Steel Tube Beam-Columns. Journal of Structural Engineering 2002; 128(3):309-318.

[17] Varma A H, Ricles J M, Sause R, et al. Seismic Behavior and Design of High-Strength Square Concrete-Filled Steel Tube Beam Columns. Journal of Structural Engineering 2004; 130(2):169-179.

[18] Skalomenos K A, Hayashi K, Nishi R, et al. Experimental behavior of concrete-filled steel tube columns using ultrahigh-strength steel. Journal of Structural Engineering 2016; 142(9): 04016057.

[19] O'Shea M D, Bridge R Q. Design of circular thin-walled concrete filled steel tubes. Journal of Structural Engineering 2000; 126(11): 1295-1303.

[20] Zhang Y, Xu C, Lu X. Experimental study of hysteretic behaviour for concrete-filled square thin-walled steel tubular columns. Journal of Constructional Steel Research 2007; 63(3): 317-325.

[21] Goto Y, Jiang K, Obata M. Stability and ductility of thin-walled circular steel columns under cyclic bidirectional loading. Journal of structural engineering 2006; 132(10): 1621-1631.

[22] Gajalakshmi P, Helena H J. Behaviour of concrete-filled steel columns subjected to lateral cyclic loading. Journal of Constructional Steel Research 2012; 75: 55-63.